بیست و چهارمین کنفرانس اپتیک و فوتونیک و دهمین کنفرانس مهندسی و فناوری فوتونیک ایران
۱۰ الی ۱۲ بهمن ۹۶ – دانشگاه شهرکرد
24th Iranian Conference on Optics and Photonics (ICOP 2018) and
9th Iranian Conference on Photonics Engineering and Technology (ICPET 2018)
Jan 30 - Feb 1 , 2018 - Shahrekord University

خواص اپتیکی نانو ذرات کلوییدی پلاسمونی Au-MoO3 ساخته شده به وسیله کاهش مستیم نمک طلا توسط اکسید مولیبدن.

مهری السادات حسینی، مهدی رنجبر

دانشکده فیزیک، دانشگاه صنعتی اصفهان، اصفهان، صندوق پستی ۸۴۱۵۶-۸۳۱۱۱

چکیده – در این پژوهش نانو ذرات صفحه ای اکسید مولیبدن با نقص اکسیژن با استفاده از روش الکترواکسیداسیون در الکترولیت آب سنتز شدند. این محلول کلوییدی، باند جذبی پلاسمونی در ناحیه مادون قرمز در طول موج ۷۶۰ نانومتر دارد. با استفاده از محلول کلوییدی اکسید مولیبدن با استوکیومتری ناقص به عنوان عامل کاهنده و محلول نمک طلا، نانو ذرات طلا با اندازه‌ی کوچکتر از ۱۰ نانو متر ساخته شدند. تشکیل نانو ذرات طلا در بستر اکسید مولیبدن منجر به ظهور دو پیک پلاسمونی در محدوده‌ی ۵۵۰-۶۸۰ نانو متر می‌شود. جابجایی پیک پلاسمونی ناشی از تغییر ضریب شکست محلی نانو ذرات طلا در اطراف نانو صفحات اکسید مولیبدن است. ساختار بلوری و مورفولوژی نمونه ها از طریق پراش پرتو ایکس و تصویر میکروسکوپ الکترونی عبوری مورد بررسی قرار گرفته است. همچنین در بررسی پدیده‌ی رنگ زایی گازوکرومیک محلول کلوییدی به دست آمده در حضور گاز هیدروژن شاهد جابجایی پیک جذب پلاسمونی به علت تغییر ضریب شکست محلول و غلظت حامل های بار هستیم.

کلید واژه- اکسید مولیبدن، نمک طلا، نانو ذرات طلا، رزونانس پلاسمون های سطحی جایگزیده، الکترواکسیداسیون.

Optical properties of Plasmonic Au-MoO3 colloidal nanoparticles by in situ reduction of HAuCl4 by blue MoOx nanosheets

M. A. Hosseini, M. Ranjbar[1]

Department of Physics, Isfahan University of Technology, Isfahan 84156-83111, Iran

In this paper defective colloids of blue MoOx nanosheets were prepared by electro-oxidation method in water. This colloidal solution exhibits a plasmonic absorption band in the infrared region at about 760 nm. Here, we report a solution-based approach for the synthesis of colloidal gold nanoparticles (GNPs) by proposing sub-stoichiometric blue MoOx nanosheets as a reducing reagent for HAuCl4. Formation of GNPs of <10 nm in diameter in a molybdenum oxide background emerged two plasmonic peaks at 550-680 nm range. We observed a red-shift in the LSPR spectral peaks that as attributed to change in the local refractive index of gold decorate the molybdenum oxide nanosheets. Crystalline structure and morphology of samples were studied with X-ray diffraction and Transmission electron microscopy. Furthermore, we demonstrate the gasochromic coloration effect in the presence of hydrogen gas in Mo:Au solutions of affecting the LSPR absorptions. It was observed that both gold and Mo oxide plasmonic peaks have a red-shift by insertion of hydrogen gas which is attributed to change in solution refractive index and defect concentration.

Keywords: MoOx, $HAuCl_4$, gold nanoparticles, localized surface plasmon resonance, electro-oxidation.

[1] Corresponding author. Tel.: +98 31 3391 2375; fax: +98 313 391 2376. E-mail address: ranjbar@cc.iut.ac.ir (M. Ranjbar)

Introduction

Gold nanoparticles (NPs) have many applications in biological and chemical sensing due to surface plasmon resonance and negligible toxic properties [1, 2]. Synthesis of gold NPs with different shape and size has become one of the most interested research topics now. Gold NPs are usually prepared by chemical reduction of gold precursors, commonly $HAuCl_4$, with variety of reducing agents. In addition to single GNPs, much works has been devoted to synthesis of gold-metal oxide compositional NPs to enhance the chemical activity [3, 4]. Compounds of nanostructured molybdenum oxide have been intensively investigated and are regarded in various fields. The Molybdenum oxides in due to quantum size effects, allow shifts in electronic structure and oxidation potentials so that permits enhanced catalytic activities not possible in bulk. Especially in 2D materials, edge-site substitution with metals and nucleation and growth of metal NPs is possible due to the high density of defect-containing reactive edges [5]. Therefore, they may be a good candidate for use as the primary nucleus for the reduction of $HAuCl_4$. On the other hands, it is believed that surface defect sites play a key role in catalytic activity of molybdenum oxide, either as nucleation centers or as attachment sites [6]. Therefore, they may be a good candidate for use as the primary nucleus for the reduction of $HAuCl_4$. On the other hands, it is believed that surface defect sites play a key role in catalytic activity of molybdenum oxide, either as nucleation centers or as attachment sites [6]. Therefore, in addition to two-dimensionality, evolution of defects in molybdenum oxide nanosheets can enhance its catalytic activity toward a metal precursor and is often performed by reducing the fully oxidized MoO_3 [7]. In this paper we found that the blue molybdenum oxide is able to form Au NPs with pronounce LSPR properties. Herein, we report the experimental studies by UV-Vis spectrometry, XRD and TEM. The produced Au-MoO3 colloidal NPs are also able to exhibit gasochromic coloration property with a spectral shifting aspect in the presence of hydrogen gas

1. Experimental

Colloidal NPs of molybdenum oxide were fabricated via an electrochemical anodizing of molybdenum sheets in a 0.02 M HCl electrolyte (Fig.1). In this process, two molybdenum sheets were put 1 cm apart from each other. A 30 V DC bias voltage was applied to the two ends of sheets for 5 min. By applying voltage, the anode began to corrode electrochemically, gradually dispersed into the electrolyte and a colloidal solution was obtained. By merely mixing of hydrogen tetrachloroaurate (III) hydrate solution (10^{-4} Molar) with the colloidal molybdenum oxide, samples of different MoO_x: HAuCl4 ratios (Mo:Au =10:1, 20:1, 30:1 and 40:1) were obtained (Fig 1). They were named according to the Mo: Au ratio (for example $MA_{10:1}$ denotes Mo:Au(10:1). To characterize samples optical absorptions, x-ray diffraction, TEM imaging and XPS analysis were done. Gasochromic coloration experiments were conducted by injection of 10% H2/Ar mixed gas. To do this, a tiny glass pipe was inserted into a sealed quartz cell containing the solution.

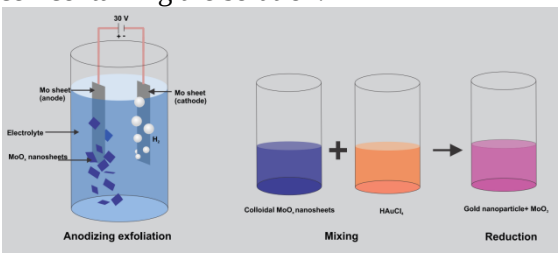

Fig 1: Schematic representation of anodizing exfoliation of Mo sheets and obtaining blue MoO_x nanosheets, mixing with $HAuCl_4$ process and formation of Au+MoO_3

2. Result and discussion

Fig.2 (a) illustrates the optical absorption spectra of the $HAuCl_4$ solution, as-prepared blue MoO_x colloids before and after mixing with the $HAuCl_4$ in four different Mo:Au ratios of 10:1, 20:1, 30:1 and 40:1. For the spectrum of blue MoO_x in Fig.2(a), the plasmonic behavior concerns a broad optical absorption band observable in the NIR region at ~760 nm, which originates from the presence of oxygen vacancies [8] and as a metal oxide semiconductor, it represents an absorption edge under 400 nm due to excitation across the optical band gap. Furthermore, the $HAuCl_4$ has a characteristic peak around 300 nm. As can be seen, the mixing of these two solutions results in formation of gold plasmon absorption peak at about 550 nm, indicating the gold precursor reduces to GNPs which can also be viewed from the appearing a pink color in the photographic image. In addition, the $HAuCl_4$ peak decays for all the mixing ratios after the mixing process, thus indicating the gold precursor decomposes completely. Formation of GNPs is understandable according to diffraction gold diffraction peaks in the XRD patterns. The XRD patterns of the initial blue MoO_x, samples $MA_{10:1}$ and $MA_{40:1}$ are shown in Fig.2 (b). No diffraction peak exists over the pattern of MoO_x in part (b), which will be explained by two-dimensionality of the MoO_x

nanoflakes (TEM images, Fig. 3). However, apparent diffraction peaks of fcc Au (JCPDS No. 00-001-1172) appears for samples $MA_{10:1}$ and $MA_{40:1}$. The sharpest peak at (111) direction suggests that Au NPs are likely more developed along this direction [9].

The gold absorption wavelength (~550 nm) in Fig.2 suggests that the particle size should be smaller than 20 nm [32] in agreement with the TEM results in the next section. Moreover, gold plasmon peak position demonstrates blue-shift by increasing the Mo:Au ratio. This spectral shift is mainly attributed to a reaction-induced variation in the solution refractive index, where the gold peak position can be used as an indicator for environment refractive index according to the following equation [10]:

$$\lambda_{max} = \lambda_p \sqrt{1 + 2n_m^2} \quad (1)$$

In which λ_{max} is the gold peak position, λ_p is bulk plasmon resonance wavelength and n_m is refractive index of the medium.

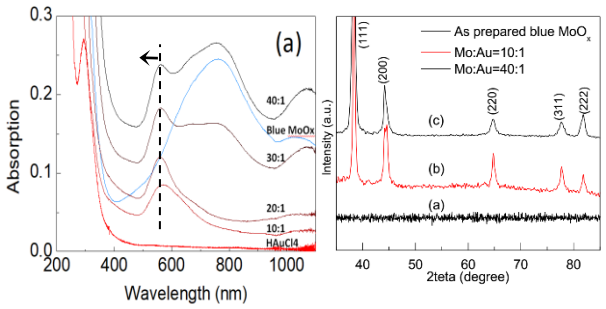

Fig.2: (a) Optical absorption spectra of initial blue MoO_x nanosheets colloidal solution, $HAuCl_4$ solution and after their merely mixing at different Mo:Au ratio of 10:1, 20:1, 30:1 and 40:1. (b) XRD patterns of initial MoO_x nanosheets, sample $MA_{10:1}$ and sample $MA_{40:1}$

TEM images are shown in Fig.3 (a, b) for the initial blue MoO_x, and sample $MA_{40:1,}$ respectively. The two dimensional nature of MoOx colloids is identified from the TEM image in part (a) where most of observable flakes look transparent, thus indicating that their thickness is only few nanometers. This is probably why there are no peaks in the XRD patterns. An average lateral size of 24 nm was measured for the nano-flakes. In TEM image of sample $MA_{40:1}$ (part (b)) two different kinds of particles exist. Those few particles that are bigger and seem darker are attributed to MoO3 while those of smaller dimension are attributed to GNPs. One can see that these GNPs are uniformly distributed and the gold averages size is ~4.5 nm in sample $MA_{40:1}$, consistent with LSPR wavelength position in the absorption spectra Partial formation of core-shell structure is also expectable because insets of Fig.3 reveal a core-shell structure with about 4 nm.

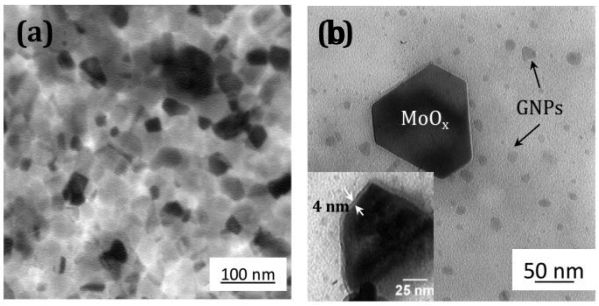

Fig.3: TEM images (a) initial MoOx nanosheets, (b) sample $MA_{40:1}$

The Au-MoO_x colloids, made by the reduction method of this paper, exhibited a considerable gasochromic response in which a color change from transparent to blue occurs upon bubbling %10 hydrogen gas. In Fig.4, spectral time variations for Mo:Au ratios of 10:1 and 40:1, are displayed at time intervals of 15 min. Before gas injection, the gold LSPR peaks dominate the spectrum, while there is no significant absorption in the NIR region. Upon exposure to 10% H2/Ar at room temperature, drastic rise in the absorption peak occurs in the NIR region for all the samples, which demonstrate formation of the MoO_x LSPR peak. Usually, the gasochromic developing process takes few minutes and a change from colorless to blue color can be observed during gas exposure, even after cutting off the gas exposure. Photographic images in Fig.4 show that the pink color of Au-MoO_3 sample turns blue after hydrogen injection in a sealed quartz cell. This gasochromic behaviour has been related to the reduction of Mo by hydrogen atoms spilt-over [11] and as a result, oxygen defect develops into the Mo oxide lattice and the fully oxidized particles recover the $MoO_{x<3}$ composition. Partial reduction of Mo^{6+} cations to Mo^{5+} is also expected according to $MoO_3 + (3\text{-}x)\ H_2 \rightarrow MoO_x + (3\text{-}x)$ H2O reaction. The gold NPs in these systems can promote the room temperature dissociation of H_2 into H atoms and accelerate the coloration of Mo oxide colloids. The gold LSPR curve is integrated as a shoulder into the spectrum. It can be clearly seen that with the colouring time, the LSPR peak of molybdenum oxide dominates the spectrum and its intensity increases with Mo:Au ratio. As the intensity of Mo oxide plasmonic peak increases upon gas exposure, the LSPR curve of gold shifts about towards red wavelengths, which implies that the resonance wavelength increases. This noticeable red-shift,

shown in the Fig.4, for gold plasmonic peak is about 20 nm for sample $MA_{10:1}$. As before, this red-shift is due to the change in the dielectric constant in the solution on exposure to gas because the electrical, chemical and optical properties of Mo oxide change in the presence of hydrogen. This is probably accompanied by an increase in the refractive index of the solution environment (gold surrounding) due to the coloration of molybdenum oxide. Another LSPR red-shift is observed for Mo oxide plasmonic peak after interacting with hydrogen gas, which is remarkably high (about 50 nm). This shifting is shown in sample $MA_{40:1}$ with arrows. In the case of plasmonic metal oxides, not only the shape, size, and environment of the NPs affect the location of the peak, but also the level of oxygen defects is also effective in such a way that the wavelength reduces by defect concentration [12]. Therefore, the observed red shift can be partially due to the difference in the concentration of defects in the initial defective blue colloids obtained in exfoliation process and those created in the hydrogen gasochromic coloration process.

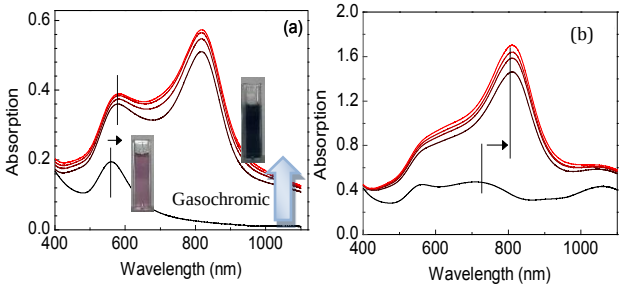

Fig.4: (a) Spectral time variations of Au-Mo oxide samples in the gasochromic process for Mo:Au ratios of 10:1 and (b)sample of 40:1, at hydrogen (10%) injection time intervals of 15 min.

The formation of Au-MoO_3 via reduction mechanism is considered as the follows. The blue MoO_x nanosheets obtained by anodizing exfoliation have a lot of surface defect sites. Localized electrons in oxygen vacancy sites transfer to the positively charged gold ions, oxidizing MoO_x and reducing gold ions to gold metal and gold nuclei formation, which are responsible for the formation of gold plasmonic peak and decay of MoO_x peak. So two-dimensionality and defects in our MoO_x play a key role in its reducing ability. On the other hands, coloration in the gasochromic process is attributed to defect reformation via hydrogen injection and oxygen removing from the MoO_3. When the initial MoO_x blue color disappears, it is an oxidizing effect because it is known that fully oxidized MoO_3 colloids are colorless and the blue color of defect-containing molybdenum oxide compounds is correlated to the oxygen defects. According to the literature, Mo^{5+} is commonly accepted to be responsible for the blue color and absorption in MoO_x [13-14]. Therefore, losing the blue color is attributed to oxidation of MoO_x which is accompanied by formation of gold metal.

3. Summary

In this paper, the blue colloidal MoOx were prepared by anodizing exfoliation method, which is a simple and fast approach. Colloidal nanoparticles have a plasmonic absorption peak at about 760 nm. Based on UV-vis spectrometry, TEM and chemical analysis, these colloidal nanosheets were able to reduce $HAuCl_4$ to GNPs of several nanometers in size, while they themselves were oxidized and loss their plasmonic peak. The resulting nanoparticles exhibited gasochromic coloration effect in the presence of hydrogen gas. In this process, the absorption peak of molybdenum oxide raise again and its relative intensity was enhanced by increasing the amount of molybdenum oxide. Also, in this process we observed a red-shift in the gold peak, which was attributed to an increase in the refractive index due to the change in the oxidation state of molybdenum oxide.

4. References

[1] D.A. Giljohann, D.S. Seferos, W.L. Daniel, M.D. Massich, P.C. Patel, C.A. Mirkin, International Edition 49(19) (2010) 3280-3294.
[2] X. Huang, P.K. Jain, I.H. El-Sayed, M.A. El-Sayed, Medical Science 23(3) (2008) 217-228.
[3] M. Murdoch, G. Waterhouse, M. Nadeem, J. Metson, M. Keane, R. Howe, J. Llorca, H. Idriss, Nature Chemistry 3(6) (2011) 489-492.
[4] V. Subramanian, E.E. Wolf, P.V. Kamat, Journal of the American Chemical Society 126(15) (2004) 4943-4950.
[5] M. Chhowalla, H.S. Shin, G. Eda, L.-J. Li, K.P. Loh, H. Zhang, Nature chemistry 5(4) (2013) 263-275.
[6] F. Wang, W. Ueda, J. Xu, Angewandte Chemie International Edition 51(16) (2012) 3883-3887.
[7] H. Bai, W. Yi, J. Li, G. Xi, Y. Li, H. Yang, J. Liu, Journal of Materials Chemistry A 4(5) (2016) 1566-1571.
[8] X. Tan, L. Wang, C. Cheng, X. Yan, B. Shen, Z Chemical Communications 52(14) (2016) 2893- 2896.
[9] W. Yan, V. Petkov, S.M. Mahurin, S.H. Overbury, S. Dai, Catalysis Communications 6(6) (2005) 404-408.
[10] V. Amendola, M. Meneghetti, Journal of Physical Chemistry C 113(11) (2009) 4277-4285.
[11] P. Castillero, V. Rico-Gavira, C. López-Santos, A. Barranco, V. Pérez-Dieste, C. Escudero, J.P. Espinós, A.R. González-Elipe, The Journal of Physical Chemistry C 121(29) (2017) 15719-15727.
[12] J.M. Luther, P.K. Jain, T. Ewers, A.P. Alivisatos, Nature materials 10(5) (2011) 361.
[13] R.S. Patil, M.D. Uplane, P.S. Patil Applied Surface Science 252(23) (2006) 8050-8056.
[14] J. Jiang, J. Liu, S. Peng, D. Qian, D. Luo, Q. Wang, Z. Tian, Y. Liu, Journal of Materials Chemistry A 1(7) (2013) 2588- 2594.